 Human Molecular Genetics, 1997, Vol. 6, No. 2 157–164

ARTICLE

# Point mutations and an intragenic deletion in *LIS1*, the lissencephaly causative gene in isolated lissencephaly sequence and Miller–Dieker syndrome

**Cristiana Lo Nigro[1,2,+], Samuel S. Chong[3,4,+], Ann C. M. Smith[3], William B. Dobyns[5], Romeo Carrozzo[2] and David H. Ledbetter[3,*]**

[1]Laboratorio di Genetica Molecolare and [6]Servizio di Genetica Medica, San Raffaele Hospital, Milan, Italy, [2]Telethon Institute of Genetics and Medicine, San Raffaele Biomedical Science Park, Milan, Italy, [3]National Center for Human Genome Research, National Institutes of Health, Bethesda, MD 20892, USA, [4]Department of Pediatrics, Georgetown University Medical Center, Washington, DC 20007, USA and [5]Division of Pediatric Neurology, Departments of Neurology and Pediatrics, University of Minnesota Medical School, Minneapolis, MN 55455, USA

Received September 18, 1996; Revised and Accepted November 18, 1996 DDBJ/EMBL/GenBank accession nos U72333–U72342

**Classical lissencephaly (smooth brain) or generalized agyria-pachygyria is a severe brain malformation which results from an arrest of neuronal migration at 9–13 weeks gestation. It has been observed in several malformation syndromes including Miller–Dieker syndrome (MDS) and isolated lissencephaly sequence (ILS). A gene containing β-transducin like repeats, now known as *LIS1*, was previously mapped to the ILS/MDS chromosome region on 17p13.3. We recently localized the classical lissencephaly critical region to the *LIS1* gene locus by molecular analysis of key ILS and MDS patients. We have now characterized the structure of *LIS1*, which consists of 11 exons, and have searched for the presence of subtle mutations in 19 ILS patients who showed no gross rearrangements of *LIS1*. Single strand conformational polymorphism (SSCP) analysis revealed band-shifts for three patients, each involving a different coding exon, which were not observed in their respective parental DNAs. Sequence analysis identified these *de novo* mutations as a dA→dG transition in exon VI at nucleotide 446, a dC→dT transition in exon VIII at nucleotide 817, and a 22 bp deletion at the exon IX–intron 9 junction from nucleotide 988 to 1002+7, which causes skipping of exon IX in the mature LIS1 transcript. These changes are predicted to result in an H149R amino acid substitution, an R273X premature translation termination, and abolition of amino acids 301–334, in the respective LIS1 proteins. These data thus confirm *LIS1* as the gene responsible for classical lissencephaly in ILS and MDS.**

## INTRODUCTION

Classical lissencephaly (smooth brain) or generalized agyria-pachygyria is a severe brain malformation caused by an arrest of neuronal migration at 9–13 weeks gestation and is characterized by a smooth cerebral surface, abnormally thick and poorly organized cortex with four primitive layers, diffuse neuronal heterotopia, enlarged and dysmorphic ventricles, and often hypoplasia of the corpus callosum (1,2). It has been observed in several different malformation syndromes including Miller–Dieker syndrome (MDS), isolated lissencephaly sequence (ILS), and X-linked lissencephaly and subcortical band heterotopia (XLIS) (3,4).

MDS consists of classical lissencephaly (always grade 1 or 2), characteristic facial abnormalities, and sometimes other birth defects (5). The facial changes include prominent forehead, bitemporal hollowing, short nose with upturned nares, flat midface, protuberant upper lip, thin vermillion border of the upper lip and small jaw. Some patients have a small midline calcification in the region of the corpus callosum or septum pellucidum. ILS consists of classical lissencephaly (grades 1–4) and normal facial appearance or subtle facial changes reminiscent of MDS but not sufficient for diagnosis (2). Many patients have minor facial changes such as small jaw and bitemporal hollowing. The brain malformation is more variable than in MDS (grades 1–4 with grades 2–3 most common). Other birth defects are rare.

*To whom correspondence should be addressed at: Center for Medical Genetics, The University of Chicago, 5841 South Maryland Avenue, MC 2050, Chicago, IL 60637-1470, USA. Email: dhl@babies.bsd.uchicago.edu
+Both authors contributed equally to this work, and are listed in alphabetical order.

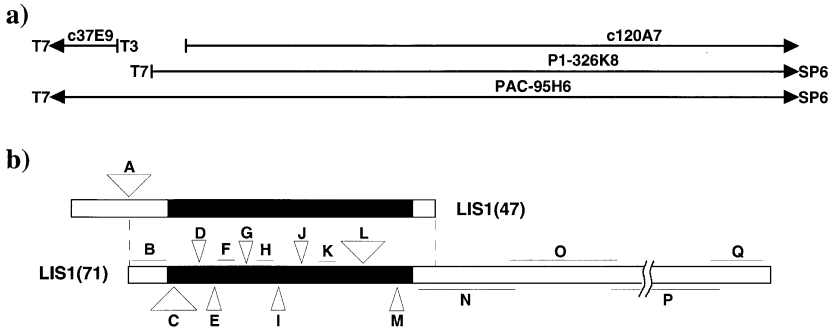


**Figure 1.** (**a**) Schematic of *LIS1*-containing cosmid, P1 and PAC clones (not drawn to scale) and (**b**) orientation and alignment of the LIS1 cDNAs with respect to these genomic clones. Where determined, direction of the T7, T3, and SP6 ends of genomic clones are indicated. In (b), capitalized letters refer to results of PCR amplification of genomic clones using primers obtained from LIS1 cDNA sequences (cross-referenced in Table 1). Horizontal lines depict genomic amplification product of similar size to cDNA. Small triangles depict products that are larger than cDNA, and large triangles indicate absence of amplification product, suggestive of large intronic sequences.

Our previous studies demonstrated that almost all children with MDS have cytogenetically visible or submicroscopic deletions in chromosome 17p13.3, while about one third of children with ILS have submicroscopic deletions of the same region which most often involve marker *D17S379* (6). These results suggested that haploinsufficiency of a gene in this region was responsible for the defect in neuronal migration. During a search for genes containing G protein β-subunit (β-transducin-like) repeats, a novel gene now known as *LIS1* was isolated and mapped to chromosome 17p13.3 (7). Apparently partial and non-overlapping deletions were detected in one ILS and one MDS patient (although first reported as two MDS patients), which suggested that this gene was responsible for both lissencephaly and the facial abnormalities characteristic of MDS (7). We later discovered that one of the cDNA clones used in the initial characterization of the 5′ end of *LIS1* was chimeric (8).

Our subsequent analyses of key translocation and deletion patients using newly isolated probes, including the correct 5′ end of *LIS1*, have allowed us to revise the *LIS1* gene boundaries, and reduce the chromosome 17 lissencephaly minimal critical region to the *LIS1* locus. These results showed that mutations of *LIS1* are not responsible for the facial abnormalities or other manifestations of MDS (9). We have now characterized the structure of the *LIS1* gene, and identified subtle *de novo* mutations in three ILS patients for whom no gross rearrangements were detectable by fluorescence *in situ* hybridization (FISH) or Southern analyses.

## RESULTS

### Structure of the *LIS1* gene

A genomic contig of ~500 kb encompassing the *LIS1* gene was generated in the lissencephaly critical region in 17p13.3, and several cosmid, P1 and PAC clones were shown to contain portions of or the entire *LIS1* gene (9). Of these, we used c37E9, c120A7, P1-326K8, and PAC-95H6 for characterization of *LIS1* (Fig. 1a).

Putative exon–intron boundaries were first determined by PCR amplification of one or more of these genomic clones using cDNA-derived primers, and comparing the genomic amplicon sizes against the expected cDNA sizes. A genomic PCR product equivalent in size to cDNA implied the absence of an intron between the primer sequences. Conversely, a larger genomic PCR product indicated the presence of intronic sequences between the primer locations. Finally, the complete absence of any product was also taken to suggest the presence of intervening sequences that were too large to be amplified. Table 1 lists the primers, reagents, cDNA sizes and results of the genomic PCR analysis. Positions of the putative introns inferred from this analysis are illustrated in Figure 1b.

These genomic clones were then directly sequenced using primers listed in Table 2 in order to obtain exon–intron junctional sequences. The sequence data obtained were in agreement with

**Table 1.** Analysis of *LIS1* gene structure by PCR of genomic templates using LIS1 cDNA primers

| Primer | Sequence (5' - 3') | $T_m$ (°C) | cDNA Size | Genomic Template | PCR Product* (Size) |
|---|---|---|---|---|---|
| LIS1(47)51F | CGAGCGCCGAGCTTGGACTC | 70 | 428 bp | 1 | A |
| LIS1(47)478R | CTCGTTGTCTCTGGGACAGCACCA | 70 | | | (n.p.) |
| LIS1(71)24F | TCCGGTGGAATGAATCTTAC | 60 | 192 bp | 1, 2 | B |
| LIS1(71)215R | TGGCTGTAATGTCAAGCTTATC | 60 | | | (~0.2 kb) |
| LIS1(71)103F | TGTGGAAGACACTTAGTGGCATA | 60 | 156 bp | 1, 3 | C |
| LIS1(71)285R | CCATTTGAACGAAGATAATCTGC | 60 | | | (n.p.) |
| LIS1(71)269F | TATCTTCGTTCAAATGGCTATGAAG | 60 | 103 bp | 1, 2 | D |
| LIS1(71)371R | CCAAAAGACCAGCATACTTTTTATC | 60 | | | (~0.7 kb) |
| LIS1(71)361F | TGGTCTTTTGGAAAAAAAATGG | 60 | 145 bp | 1, 2 | E |
| LIS1(71)505R | GGGAATCCATTCTTTTGGGT | 60 | | | (~1 kb) |
| LIS1(71)442F | AAAAGAAGAATTTACGTCAGGTGG | 60 | 103 bp | 1, 2 | F |
| LIS1(71)544R | ACTCCTGTGACCACTCAATGC | 60 | | | (~0.1 kb) |
| LIS1(71)442F | (as above) | 60 | 284 bp | 1, 2 | G |
| LIS1(71)726R | CAGAACAGGAAGCCAGAAGC | 60 | | | (~2 kb) |
| LIS1(71)624F | ATTATGAGACTGGAGATTTTGAACG | 60 | 102 bp | 1, 2 | H |
| LIS1(71)726R | (as above) | 70 | | | (~0.1 kb) |
| LIS1(71)677F | CAGGACATTTCATTCGACCACAGCG | 70 | 155 bp | 3 | I |
| LIS1(71)831R | TCTCCATTGGGCATGATGGCTACTG | 70 | | | (~3 kb) |
| LIS1(71)802F | TTCTTCAGTAGCCATCATGCC | 60 | 198 bp | 1, 2 | J |
| LIS1(71)999R | CATACACGCACAGTCTGGTCATTG | 60 | | | (~2 kb) |
| LIS1(71)1001F | GTCGTAGCAACAAAGGAATGC | 60 | 102 bp | 1, 2 | K |
| LIS1(71)1102R | TTCAGAGATGGAGGAATATGAGC | 60 | | | (~0.1 kb) |
| LIS1(71)1001F | (as above) | 60 | 445 bp | 1, 2 | L |
| LIS1(71)1445R | GGCACTCCCACACTTTTACTG | 60 | | | (n.p.) |
| LIS1(71)1324F | CAAGCGATGCATGAAGACC | 60 | 122 bp | 2 | M |
| LIS1(71)1445R | (as above) | 60 | | | (~1.5 kb) |
| LIS1(71)1449F | GATTGTGTCTCCTTCGGCC | 60 | 373 bp | 2 | N |
| LIS1(71)1821R | CAGGCACCAACAGATAGCAG | 60 | | | (~0.35 kb) |
| LIS1(71)1718F | AAGTTGAATCAATTGAACTAGGGC | 60 | 793 bp | 1, 2 | O |
| LIS1(71)2510R | GCACGCTCCATTAAACCCTG | 60 | | | (~0.8 kb) |
| LIS1(71)2387F | GTGTGCCCATTTGAAAGGAGTG | 60 | 2.56 kb | 2 | P |
| LIS1(71)4947R | AGAGTGAGCTTTAGGGATGCC | 60 | | | (~2.5 kb) |
| LIS1(71)4846F | GTCACGGCTGGACTGAATG | 60 | 322 bp | 2 | Q |
| LIS1(71)5167R | GCAACAAATCTTACTGTAAAACACG | 60 | | | (~0.3 kb) |

Where $T_m$ of primers are different, the lower $T_m$ was used in the PCR. Templates: 1, PAC-95H6; 2, P1-326K8; 3, c120A7 (see also Fig. 1a).
*Capitalized letters refer to the corresponding segments in Figure 1b.
n.p.: no amplification product.

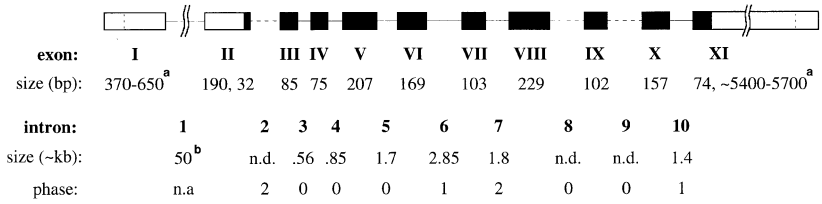


**Figure 2.** Schematic representation of *LIS1* gene structure (not drawn to scale). Exons are depicted as boxes and numbered with Roman numerals. Filled-in regions indicate translated portions of the gene. Introns are indicated by horizontal lines and numbered with arabic numerals. Dotted lines depict undetermined intron sizes. Intron phase describes interruption of the reading frame between codons (0), between the first and second nucleotides of a codon (1), or between the second and third nucleotides of the codon (2). [a]Sizes of the first and last exons are indicated as a range, since the LIS1 transcriptional start site/s have not been precisely mapped. [b]Approximate size of intron 1 as determined by Southern analysis of PAC clones 95H6 and 308F9 (ref. 9). n.d., not determined; n.a., not applicable.

**Table 2.** Primers used to sequence *LIS1* exon/intron boundaries

| Primer | Sequence (5' - 3') | Template | Sequence obtained |
|---|---|---|---|
| LIS1(47)51F | (Table 1) | c37E9 | exon I / intron 1 |
| SCOS1-T3* | CCGCAATTAACCCTCACTAAAGG | c37E9 | intron 1 / exon I |
| LIS1(71)120R | CACTAAGTGTCTTCCACACAGG | P1-326K8 | intron 1 / exon II |
| LIS1(71)103F | (Table 1) | P1-326K8 | exon II / intron 2 |
| LIS1(71)285R | (Table 1) | P1-326K8 | intron 2 / exon III |
| LIS1(71)269F | (Table 1) | c120A7 | exon III / intron 3 |
| LIS1(71)371R | (Table 1) | c120A7 | intron 3 / exon IV |
| LIS1(71)361F | (Table 1) | c120A7 | exon IV / intron 4 |
| LIS1(71)505R | (Table 1) | c120A7 | intron 4 / exon V |
| LIS1(71)519F | AATATGCATTGAGTGGTCACAGG | c120A7 | exon V / intron 5 |
| LIS1(71)649R | TCGTTCAAAATCTCCAGTCTCAT | c120A7 | intron 5 / exon VI |
| LIS1(71)706F | GCTTCTGGCTTCCTGTTCTG | c120A7 | exon VI / intron 6 |
| LIS1(71)839R | CTATATGATCTCCATTGGGCATG | c120A7 | intron 6 / exon VII |
| LIS1(71)805F | TTCAGTAGCCATCATGCCCAATGGA | c120A7 | exon VII / intron 7 |
| LIS1(71)999R | (Table 1) | c120A7 | intron 7 / exon VIII |
| LIS1(71)1080F | GCTCATATTCCTCCATCTCTGAA | c120A7 | exon VIII / intron 8 |
| LIS1(71)1186R | CCACATCTTAATAGTCTTGTCTCTGG | c120A7 | intron 8 / exon IX |
| LIS1(71)1142F | CCATTCTTGCTGTCTGGATCC | c120A7 | exon IX / intron 9 |
| LIS1(71)1329R | CGCTTGTTCTTGTAATCCCATAC | c120A7 | intron 9 / exon X |
| LIS1(71)1250F | CTGTTCCATTCTGGGGGG | c120A7 | exon X / intron 10 |
| LIS1(71)1445R | (Table 1) | c120A7 | intron 10 / exon XI |

Primers ending with 'F' anneal to the antisense strand whereas primers ending with 'R' anneal to the sense strand.
*This primer anneals to the T3 end of c37E9 and was used to sequence from intron 1 into exon I (see also Fig. 1a).

the PCR analyses, with the exception of result 'L' (Table 1, Fig. 1b) where subsequent sequencing revealed the presence of two introns between the PCR primers (introns 8 and 9 in Fig. 2).

The combined PCR and sequencing analyses thus identified 11 exons in the *LIS1* gene (Figs 2 and 3). The exact transcription start site in exon I has not been determined, although we have localized the transcription start to a region between the annealing sites of primers LIS1(P)CP7F at position –865 (according to the numbering in Fig. 3) and LIS1(P)CP8F at position –558, (see figure 2 of ref. 9). All splice junctions exhibit a high similarity to the consensus sequences for donor and acceptor sites (Fig. 3; 10,11). The size of most introns could be estimated from PCR amplification of genomic templates, while we did not characterize further those introns that could not be amplified. Intron 1, however, is estimated to be ~50 kb in size based on Southern blot analyses of PAC digests using LIS1-containing cDNA and genomic probes (9).

The presence of two major LIS1-specific transcripts of ~7.5 and ~5.5 kb (9) indicates that they can arise either by alternative splicing of internal exons or by differential polyadenylation in the 3′ untranslated region (UTR) of the gene. Since several AATAAA as well as other potential polyadenylation signals are located in the 3′ UTR of cDNA clone 71, and cDNA clone 47 is polyadenylated at the first AATAAA signal of the 3′ UTR (7), we tested the latter possibility by performing northern analysis of poly(A)$^+$ RNA samples from adult brain tissues using probes corresponding to two different regions of the LIS1 3′ UTR. Using a 252 bp probe which lies 2.2–2.45 kb downstream of the translation stop (Fig. 4a, probe A), both the ~7.5 and ~5.5 kb transcripts were detected (Fig. 4b). However, only the ~7.5 kb transcript was detected when a 322 bp probe (probe B) lying 3.4–3.7 kb downstream of the translation stop was used instead (Fig. 4c). These results confirm that the two LIS1 transcripts arise by differential polyadenylation in the 3′ UTR of the *LIS1* gene. We have not determined which of the consensus or potential polyadenylation sites are utilized for either transcript, but the results nonetheless make it unlikely that additional internal exons exist in the large intron 1 or in introns 8 and 9 of *LIS1*.

## SSCP analysis of *LIS1* exons in ILS patients

The DNA of 19 ILS patients was analyzed for the presence of gross rearrangements, and subsequently for more subtle mutations, of the *LIS1* gene. All had typical manifestations of ILS by brain imaging studies and clinical exams. No submicroscopic rearrangements in 17p13.3 could be detected in any of these patients, as determined by FISH analysis of metaphase chromosomes using *LIS1* genomic probes (data not shown). Southern analysis was next performed on patient DNAs digested with four different restriction enzymes, using three cDNA probes which together encompass the open reading frame (ORF) of the gene. No altered hybridization band could be detected for any of the patients using any of these probes (data not shown).

We therefore performed an exon by exon SSCP analysis of these patients to search for subtle mutations within the *LIS1* gene. Primers for SSCP analysis were designed to amplify each coding exon separately. Given the complete sequence identity between the ORFs of *LIS1* and the homologous *LIS2* gene which maps to chromosome 2p11.2 (12), primers for each exon were first tested on DNAs from human–rodent somatic cell hybrids containing only human chromosome 2 or only human chromosome 17. Only those intronic primers amplifying DNA exclusively from the chromosome 17-only hybrid were subsequently employed. The primer sequences used in exon amplifications are listed in Table 3.

Three patients showed an electrophoretic migration band-shift in addition to the normal migrating bands, indicative of allele heterozygosity (data not shown). In patient ILS-087, the band-shift occurred in exon VI, while band-shifts were seen for exons VIII and IX in ILS-016 and ILS-079, respectively (Table 3). Confirmatory PCR amplifications and SSCP analyses were repeated for these samples to rule out the possibility of *Taq* polymerase-induced PCR artifact as a cause of these band-shifts. For all three patients, band-shifts were not detected from their respective parental DNAs, indicating that the observed changes were *de novo*.

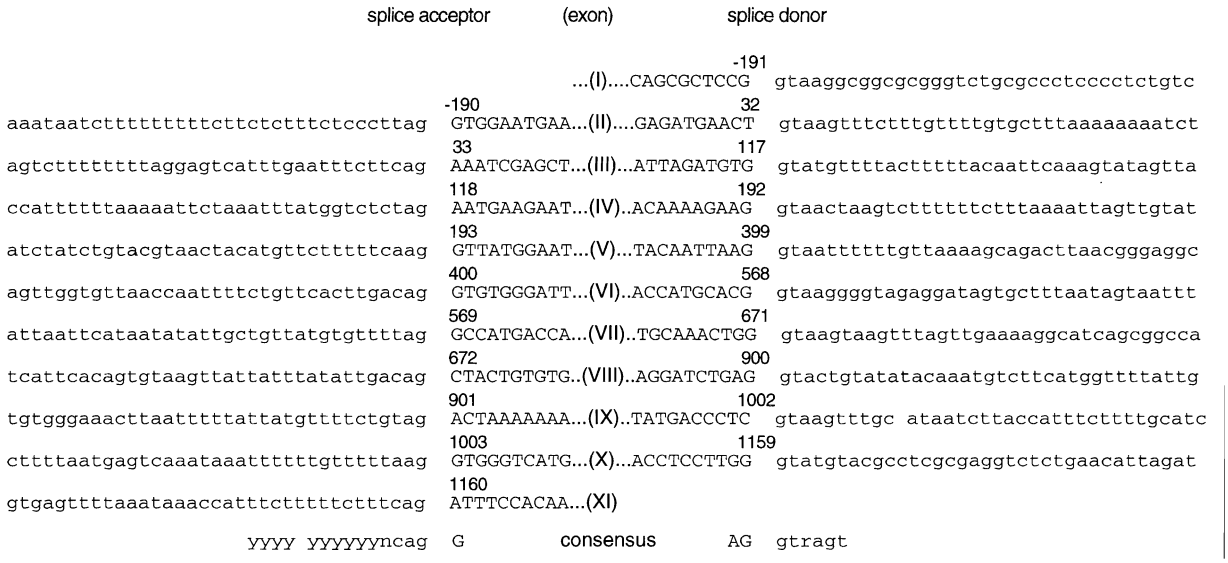


**Figure 3.** Exon–intron boundaries of *LIS1* determined from sequence analysis of genomic clones (cross-referenced in Table 2). Splice acceptor and splice donor junction sequences for the 11 exons of *LIS1* are shown. Boundaries are numbered with position +1 as the first nucleotide of the translation start.

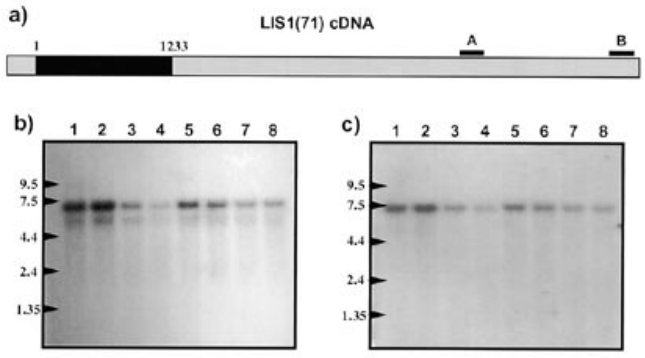


**Figure 4.** Northern blot analysis showing differential 3′ polyadenylation of the *LIS1* gene. A human multiple brain tissue blot was hybridized first with probe A (**a**), which detects the two major LIS1 transcripts of ~7.5 and ~5.5 kb (**b**). After probe removal, the same blot was rehybridized with probe B. Only the ~7.5 kb transcript is detected with the second probe (**c**). 1, cerebellum; 2, cerebral cortex; 3, medulla; 4, spinal cord; 5, occipital pole; 6, frontal lobe; 7, temporal lobe; 8, putamen.

**Table 3.** Results of SSCP analysis of LIS1 coding exons from 19 non-deletion ILS patients

| Exon | Primer | Sequence (5' - 3') | $T_m$ (°C) | Amplicon size (bp) | SSCP result (patient ID) |
|---|---|---|---|---|---|
| I | LIS1(71)103F | (Table 1) | 60 | 236 | no shift |
| | LIS1g334R | AAGAGACCTCCCAAAGCTGTA | | | |
| III | LIS1g850F | TGAAAAGAGTATCTTCAGGGTTAATG | 57 | 230 | no shift |
| | LIS1g1120R | AAAATTGTGCGTAACTGTTAACTACA | | | |
| IV | LIS1g1535F | TTGTCTTGAGGATCATAGTTAAGCC | 57 | 207 | no shift |
| | LIS1g1742R | TGCAGAAGAATGTTATTTTCAGAA | | | |
| V | LIS1g2285F | GAAATCTATCTGTACGTAACTAC | 57 | 497 | no shift |
| | LIS1g2772R | ATCACACGTTTCAGAGTACCTCC | | | |
| VI | LIS1g3166F | AAGGAGTGATGGAGTTGGTGTT | 60 | 302 | shift |
| | LIS1g3468R | GGGACACTGTACACTGTTAG | | | (ILS-087) |
| VII* | LIS1g3935F | AACCCCATGGTAAAATCCCAT | 57 | 225 | |
| | LIS1g4770R | GCCGCGTGATGCCTTTTCAACTA | | | |
| | LIS1g4553F | GGTAAAATCCCATGGTCAATTG | 57 | 205 | no shift |
| | LIS1g4758R | TTTTCAACTAAACTTACTTAC | | | |
| VIII | LIS1g5256F | ACTTCTGGGAAGTGTCCTGATG | 57 | 294 | shift |
| | LIS1g4379R | TTCAGATATCAGCAATAAAACCATG | | | (ILS-016) |
| IX | LIS1g5538F | GTCCATACCTAACTTTCTTGTGTGG | 57 | 228 | shift |
| | LIS1g5766R | CATAAAGCATTAATCCCAAAAGG | | | (ILS-079) |
| X | LIS1g6087F | AATAGATGCTATTTAAACATTTTGCC | 57 | 271 | no shift |
| | LIS1g6357R | GTTTGTCTGGCACTCCAAAATC | | | |
| XI | LIS1g5721LF | GGTCTCACTATGTTTGTTGTCCA | 60 | 173 | no shift |
| | LIS1(71)1517R | GGTATCATCAGAGTGCATCCAG | | | |

*For exon VII, the presence of an Alu repeat in the intron sequence flanking the splice-donor necessitated the use of a nested PCR strategy. LIS1g4553F and LIS1g4758R are primers nesting within LIS1g3935F and LIS1g4770R, respectively. SSCP analysis was performed on the 205 bp secondary PCR product.

## Identification of point mutations and a splice junction deletion

The shifted single-stranded fragments were isolated, re-amplified and directly sequenced on both strands. The following mutations were found: (i) a dA→dG transition at nucleotide 446 in exon VI for ILS-087, (ii) a dC→dT transition at nucleotide 817 in exon VIII for ILS-016, and (iii) a 22 bp deletion at the exon IX–intron 9 junction from nucleotide 988 to 1002+7 for ILS-079 (Fig. 5a–c). None of these DNA changes were seen in 50 unrelated controls (data not shown). The mutation in ILS-087 causes a histidine to arginine substitution at amino acid 149, whereas the mutation in ILS-016 converts an arginine at amino acid 273 into a stop codon, and would be expected to result in premature translation termination.

In ILS-079, the splice junction deletion was predicted to result in an RNA splicing error, which we confirmed by reverse transcription-PCR (RT-PCR) analysis of lymphoblastoid RNA and sequence analysis of the mutant RT-PCR product. PCR using forward primer LIS1(71)1001F, which anneals within exon VIII, and reverse primer LIS1(71)1329R, which anneals within exon X, yielded the expected fragment of 329 bp from the normal control, whereas two fragments of 329 and 227 bp were amplified from ILS-079 (Fig. 6A). Sequence analysis revealed that the entire 102 bp of exon IX was missing from the 227 bp mutant fragment (Fig. 6B). The resulting mutant protein would therefore

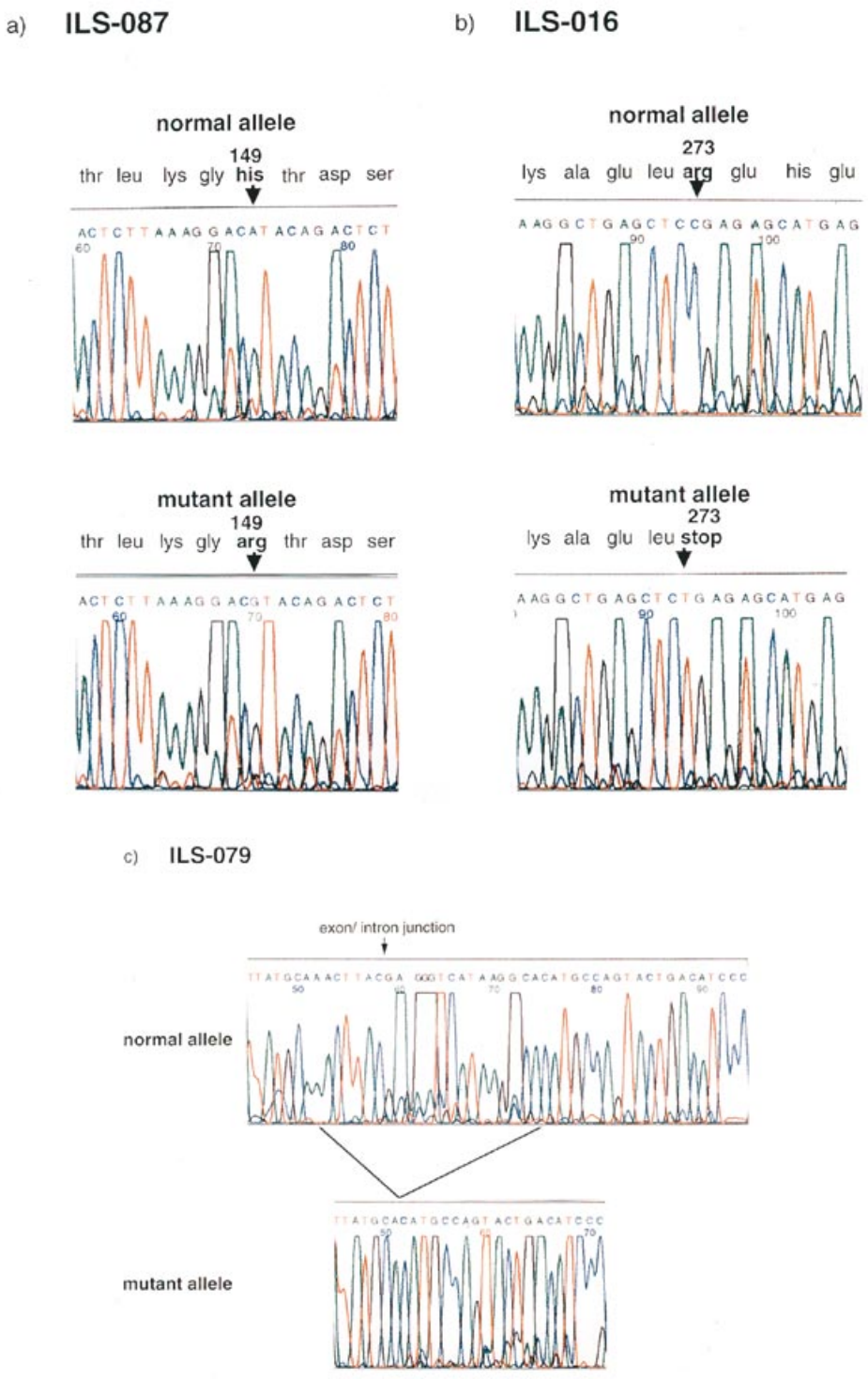


**Figure 5.** Partial *LIS1* genomic sequences comparing normal and mutant alleles of patients ILS-087 (**a**), ILS-016 (**b**) and ILS-079 (**c**). The sequences shown for ILS-079 are of the antisense strand.

be expected to contain an in-frame deletion of 34 amino acids from position 301 to 334, since introns 8 and 9 flanking exon IX interrupt the reading frame between codons (Fig. 2).

## DISCUSSION

We have characterized the structure of the *LIS1* gene, and shown that it consists of 11 exons. The average 150 bp size of the *LIS1*

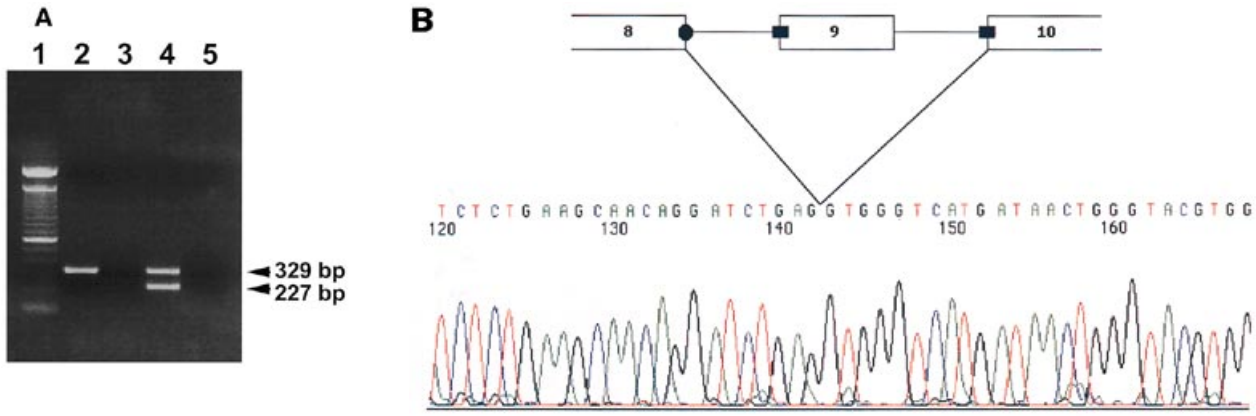


**Figure 6.** RT-PCR analysis of lymphoblastoid RNA and sequence of a 227 bp mutant LIS1 cDNA product of patient ILS-079. (**A**) Amplification results from a normal control and patient ILS-079 after reverse transcription of their respective RNAs are in lanes 2 and 4 respectively. In addition to the expected normal cDNA product of 329 bp, a smaller mutant cDNA fragment of 227 bp is detected from ILS-079. PCR reactions performed on the same RNAs, but without prior reverse transcription, are shown in lanes 3 and 5, respectively. Lane 1, 100 bp ladder size marker (Gibco-BRL). (**B**) The sequence of the smaller cDNA fragment reveals loss of 102 bp corresponding to exon IX of the *LIS1* gene. Above the sequence, a schematic representation of the genomic structure of exons VIII, IX and X is shown. Exons are depicted as open boxes, while lines represent introns. Solid squares and circle indicate normal or activated splice acceptors and splice donor, respectively. The postulated event leading to skipping of exon IX and generation of an aberrantly-spliced transcript is illustrated.

internal exons does not differ remarkably from the average size of 137 bp calculated for other vertebrates genes (13). The ~50 kb size of intron 1 is unusually large, and constitutes more than half the ~80 kb size of *LIS1* (7). Introns greater than 9 kb have been reported in less than 2% of all vertebrate genes, but the unusual size of this intron may be relevant for its transcriptional regulation, as already reported for other genes (13).

About one-third of ILS patients show deletions of 17p13.3 that include the *LIS1* gene, and we have localized the lissencephaly critical region to the *LIS1* gene (9). We have now identified subtle mutations within *LIS1* in three ILS patients who otherwise show no gross rearrangements of 17p13.3 or of *LIS1*. These results confirm *LIS1* as the causative gene for type 1 lissencephaly, and are compatible with the hypothesized molecular mechanism for this disease, i.e. haploinsufficiency of the LIS1 protein resulting from loss-of-function in one homolog. The point mutation leading to a premature translation stop in ILS-016, and the 22 bp deletion of the exon IX–intron 9 boundary leading to an interstitial 34 amino acid deletion in ILS-079, are likely to be disease-causing mutations in these patients. The phenotype and MRI abnormalities in patient ILS-079 are less severe than observed in most ILS patients, which suggests that either the mutant protein retains some residual activity, or the splice site mutation is compatible with production of some normal gene product. Examples of mutations abolishing the splice donor site and causing the exon preceding the affected splice site to be skipped have been reported elsewhere (14–17). Marvit *et al.* (18) proposed that cooperative interactions between ribonucleoproteins (snRNPs) may be involved in mRNA processing for exon identification, such that snRNPs are unable to bind efficaciously at a splice acceptor site unless they are also present at the splice donor site of the same exon.

In patient ILS-087, the histidine to arginine substitution (i) involves an amino acid residue that is conserved in the human, mouse and bovine proteins, (ii) produces a radical change in steric hindrance due to the loss of a hymidazolic ring, and (iii) is not present in his parents. Therefore, the DNA substitution observed in this child is likely to be the disease-causing mutation.

The *LIS1* gene encodes the 45K non-catalytic subunit of the brain isoform of platelet activating factor (PAF) acetylhydrolase, an enzyme which inactivates PAF (19). A low concentration of PAF has been shown to induce neuronal cell differentiation in culture, while high concentrations are toxic, suggesting that extracellular PAF levels may be crucial for differentiation of immature neurons and could affect their ability to initiate or continue migration (20). As the LIS1 protein is only one subunit of a trimeric enzyme complex, hemizygosity of the *LIS1* gene may lead to reduced levels of assembled, functional enzyme due to decreased cellular concentrations of the LIS1 subunit. Since PAF has been shown to evoke a dose-dependent neuronal growth cone collapse, it is possible that reduced levels of PAF acetylhydrolase allow an accumulation of PAF in the developing brain, causing the widespread collapse of neuronal growth cones, and resulting in the abnormal connectivity and blunted dendritic and axonal branching seen in this disorder (21). Moreover, PAF acetylhydrolase may not be the only multi-subunit complex containing the LIS1 protein, and it is possible that haploinsufficiency of LIS1 protein may adversely affect other cellular processes involved in neuronal migration. Interestingly, most of the candidate genes for human haploinsufficiency disorders code for proteins that are part of intermolecular complexes which may have an exact stoichiometry (22).

Mutations in other genes involved in neuronal migration disorders have been described. Several missense mutations and one nonsense mutation involving different regions of the cell-adhesion molecule L1 have been identified in patients with X-linked hydrocephalus (23). Also, mutations in the *EMX2* homeobox gene appear to be associated with severe open lip schizencephaly (24). Among five different mutations, one involved insertion of an adenosine nucleotide within the homeobox, and two abolished a splice site. Missense, nonsense and frameshift mutations in the *KAL-1* gene have also been described in patients with X-linked Kallmann syndrome, which is characterized by hypogonadotropic hypogonadism and anosmia (25,26). The predicted KAL-1 protein shares significant similarity with

neural-cell adhesion molecules, as well as with other molecules involved in neuronal migration and axonal pathfinding (25,26).

Research on the process of neuronal migration at the molecular level has only begun. The molecular mechanism underlying classical lissencephaly may shed further light in the understanding of the overall neural migration processes.

## MATERIALS AND METHODS

### Patient data and sample preparation

Children with ILS are referred to the Lissencephaly Research Project on a regular basis. Medical records and brain imaging studies are gathered and reviewed with informed consent (by WBD) to confirm the diagnosis. When possible, blood samples are obtained for molecular studies of the lissencephaly critical region. In 30–40% of patients studied, cytogenetic abnormalities have been detected by FISH analysis of metaphase spreads from lymphoblasts, using probes c37E9, c120A7 or PAC308F9 (9). The remaining ILS patients have had no detectable cytogenetic rearrangements; we have studied 19 of these patients in this study.

All 19 patients studied had classical lissencephaly and met diagnostic criteria for ILS, although the severity of the cortical malformation varied slightly. Classical lissencephaly grade 3 consists of frontal pachygyria (broad gyri) and posterior agyria (no gyri), while grade 4 consists of diffuse pachygyria only. Patients ILS-016 and ILS-087 had classical lissencephaly grade 3, profound mental retardation, and intractable epilepsy. Neither was able to walk or communicate. Patient ILS-079 had classical lissencephaly grade 4 which was more severe posteriorly, severe mental retardation, and epilepsy but was able to walk and use a few words.

Genomic DNA was prepared from peripheral blood leukocytes using the Qiagen-Blood midiprep kit (Qiagen). RNA was obtained from lymphoblastoid cells of patient ILS-079 using standard techniques (27). DNA was also extracted from human-rodent somatic cell hybrids containing only human chromosome 2 or 17, available from the NIGMS Human Genetic Mutant Cell Repository (Coriell Institute for Medical Research, Camden, NJ) under the GM numbers 11712 and 10498, respectively.

### cDNA and genomic clones

LIS1 cDNA clones 71 and 47 have been previously described (7). Cosmids, P1s and PACs used in *LIS1* PCR and sequence analyses have also been described (9).

### Gene structure characterization

Primers corresponding to sequences of LIS1 cDNAs 47 and 71 were used to perform PCR analysis on 10 ng of DNA from c120A7, P1-326K8, or PAC-95H6 in a preliminary screen for the presence of introns (Table 1). PCR amplifications were carried out in a 50 µl final reaction volume containing 0.25 mM of each dNTP, 0.2 µM of each primer and 1.25 U of *Taq* polymerase in standard PCR buffer (10 mM Tris–HCl pH 8.3, 50 mM KCl, 1.5 mM $MgCl_2$ and 0.01% gelatin). Reactions were performed in a PE480 thermal cycler (Perkin Elmer-ABI, Foster City, CA), with an initial denaturation at 95°C for 2 min, followed by 35 cycles of 95°C for 1 min, annealing for 1 min and 72°C for 2 min (see Table 1 for primer annealing temperatures).

Additional primers were designed for sequencing of the c37E9, c120A7 and P1-326K8 clones to determine exon–intron boundaries (Table 2). Sequencing was performed commercially (SeqWright, Houston, TX), and all sequence information has been deposited in GenBank (accession numbers U72333–U72342).

### Northern analysis

Probes A (252 bp) and B (322 bp) were PCR-amplified from LIS1 cDNA clone 71 using primer pairs LIS1(71)3648F (5′-AGCAAG-CGTGTCTTCCCCTG-3′)/LIS1(71)3899R (5′-TCCAGGTTG-TAGACGGACTGCTC-3′) and LIS1(71)4846F/LIS1(71)- 5167R (Table 1) respectively. PCR reactions were performed as above, with an initial denaturation at 94°C for 2 min, followed by 35 cycles of 94°C for 45 s, 57°C for 1 min and 72°C for 1 min.

Amplified products were separated on a 1.5% agarose gel in 1× TBE, gel-purified using the Qiaquick-spin kit (Qiagen, Chatsworth, CA) and labelled to high specific activity with [$\alpha$-$^{32}$P]dCTP using the DECAprime II random decamer labelling kit (Ambion, Austin, TX). Probes were hybridized to an adult multiple-tissue brain northern blot (Clontech, Palo Alto, CA) and subsequently washed according to manufacturer's instructions.

### Southern analysis

Eight µg of genomic DNA from these patients and normal individuals was digested with the restriction enzymes *Eco*RI, *Hin*dIII, *Bam*HI or *Pst*I. Southern blot analysis was performed according to standard procedures (28). Hybridization probes were PCR-amplified from LIS1 cDNA clones 47 and 71, using primer pairs LIS1(47)51F/LIS1(47)478R, LIS1(71)103F/LIS1-(71)1102R and LIS1(71)874F (5′-GGAAGTGCAAACTGGCT-ACTGTG-3′)/LIS1(71)1424R (5′-TTTGATCTACGCCTGCC-AGTG-3′) (see Table 1 for other primer sequences). Reactions were performed as above, with an initial denaturation at 94°C for 2 min, followed by 35 cycles of 94°C for 1 min, 60°C for 1 min and 72°C for 1 min. Prehybridizations and hybridizations were performed with Rapid-hyb buffer (Amersham, Arlington Heights, IL) according to the supplier instructions. Final wash was in 0.5× SSC, 0.1% SDS at 65°C for 30 min.

### 'Cold' SSCP analysis

Exons II–XI of the *LIS1* gene were screened for the presence of mutations using a previously described non-radioactive SSCP method (29) with modifications. Briefly, primer pairs were designed to anneal to intronic sequences flanking each exon. Each exon was amplified from 100 ng of genomic DNA template in a final reaction volume of 25 µl, using standard PCR conditions as described above, with the exception that 0.5 µM of each primer was used (see Table 3 for primer annealing temperatures).

Three µl of Qiagen-purified PCR product was mixed with 3 µl of loading buffer containing 0.01% bromophenol blue, 0.01% xylene cyanol and 98% formamide. Samples were electrophoresed at 200 V across 4–20% gradient polyacrylamide TBE precast gels using the Thermoflow Electrophoresis and Temperature Control System (NOVEX, San Diego, CA) and a chilled buffer recirculator to maintain a constant gel temperature of 8°C ± 0.5°C. With the exception of exon V samples, which were electrophoresed for 1.5 h, all of the other samples were electrophoresed for 2 h.

Gels were stained in a 1× solution of SYBR Green II (Molecular Probes) for 10 min and bands were visualized using

a 340 nm UV box. Whenever an altered band was observed, genomic amplification and SSCP analysis were repeated on a second DNA sample, in order to rule out *Taq* polymerase artifacts.

Non-shifted or shifted amplification products were sampled directly from the SSCP minigel, processed as described (29) and subjected to 25 additional PCR cycles. Re-amplified products were separated across a 1.5% agarose gel in 1× TBE at 10 V/cm, gel-purified, and sequenced on both strands.

### RT-PCR analysis of RNA from patient ILS-079

Five µg of total RNA from patient ILS-079 or a normal control were reverse transcribed using the Superscript Preamplification System kit (Gibco-BRL, Gaithursburg, MD) in a 20 µl reaction containing the *LIS1*-specific primer LIS1(71)1517R. Five µl of reverse-transcribed product was then PCR-amplified using 0.5 µM each of the primers LIS1(71)1001F and LIS1(71)1329R in a 25 µl volume (see Table 1, and 3 for primer sequences). Amplifications were performed in a PTC-200 thermal cycler (MJ Research, Watertown, MA), consisting of a 'hot start' of 94°C for 2 min, and 35 cycles of 94°C for 1 min, 55°C for 1 min, and 72°C for 1 min.

PCR products were separated in a 2% agarose gel in 1× TAE, and the 227 bp mutant fragment was gel purified, subcloned into pBluescript II KS(+) (Stratagene, La Jolla, CA) at the *Eco*RV site, and analyzed on an ABI 377 automated DNA sequencer (Perkin Elmer-ABI) using fluorescently-labelled M13 forward and reverse oligonucleotide primers.

## ACKNOWLEDGEMENTS

We thank Dr Massimo Zollo for sequencing the mutant RT-PCR product of patient ILS-079. This work was supported in part by a grant from the Italian Telethon (E.148) to RC.

## REFERENCES

1. Barkovich,A.J., Koch,T.K. and Carrol,C.L. (1991) The spectrum of lissencephaly: report of ten patients analyzed by magnetic resonance imaging. *Ann. Neurol.*, **30**, 139–146.
2. Dobyns,W.B., Elias,E.R., Newlin,A.C., Pagon,A. and Ledbetter,D.H. (1992) Causal heterogeneity in isolated lissencephaly. *Neurology*, **42**, 1375–1388.
3. Dobyns,W.B. and Truwit,C.L. (1995) Lissencephaly and other malformations of cortical development: 1995 update. *Neuropediatrics*, **26**, 132–147.
4. Dobyns,W.B., Andermann,E., Andermann,F., Czapansky-Beilman,D., Dubeau,F., Dulac,O., Guerrini,R., Hirsch,B., Ledbetter,D.H., Lee,N.S., Motte,J., Pinard,J-M., Radtke,R.A., Ross,M.E., Tampieri,D., Walsh,C.A. and Truwit,C.L. (1996) X-linked malformations of neuronal migration. *Neurology*, **47,** 331–339.
5. Dobyns,W.B., Curry,C.J.R., Hoyme,H.E., Turlington,L. and Ledbetter,D.H. (1991) Clinical and molecular diagnosis of Miller–Dieker syndrome. *Am. J. Hum. Genet.*, **48,** 584–594.
6. Dobyns,W.B., Reiner,O., Carrozzo,R. and Ledbetter,D.H. (1993) Lissencephaly, a human brain malformation associated with deletion of the *LIS1* gene located at chromosome 17p13. *J. Am. Med. Assoc.*, **270,** 2838–2842.
7. Reiner,O., Carrozzo,R., Shen,Y., Wehnert,M., Faustinella,F., Dobyns,W.B., Caskey,C.T. and Ledbetter,D.H. (1993) Isolation of a Miller–Dieker lissencephaly gene containing G protein β-subunit-like repeats. *Nature*, **364**, 717–721.
8. Chong,S.S., Tanigami,A., Roschke,A.V., and Ledbetter,D.H. (1996) *14-3-3*ε has no homology to *LIS1* and lies telomeric to it on chromosome 17p13.3 outside the Miller–Dieker syndrome chromosome region. *Genome Res.*, **6,** 735–741.
9. Chong,S.S., Pack,S.D., Roschke,A.V., Tanigami,A., Carrozzo,R., Smith,A.C.M., Dobyns,W.B., and Ledbetter,D.H. (1997) A revision of the lissencephaly and Miller–Dieker syndrome critical regions in chromosome 17p13.3. *Hum. Mol. Genet.*, **6**, 147–155.
10. Shapiro,M.B. and Senapathy,P. (1987) RNA splice junctions of different classes of eukaryotes: sequence statistics and functional implications in gene expression. *Nucleic Acids Res.*, **15**, 7155–7174.
11. Ohshima,Y. and Gotoh,Y. (1987) Signals for the selection of a splice site in pre-mRNA. Computer analysis of splice junction sequences and like sequences. *J. Mol. Biol.*, **195**, 247–259.
12. Reiner,O., Bar-Am,I., Sapir,T., Shmueli,O., Carrozzo,R., Lindsay,E.A., Baldini,A., Ledbetter,D.H. and Cahana,A. (1995) *LIS2*, gene and pseudogene, homologous to *LIS1* (lissencephaly 1), located on the short and long arms of chromosome 2. *Genomics* **30**, 251–256.
13. Hakwins,J.D. (1988) A survey on intron and exon length. *Nucleic Acids Res.*, **16**, 9893–9908.
14. Weil,D., Bernard,M., Combates,N., Wirtz,M.K., Hollister,D.W., Steinmann,B. and Raminez,F. (1988) Identification of a mutation that causes exon skipping during collagen pre-mRNA splicing in a Ehlers–Danlos syndrome variant. *J. Biol. Chem.*, **263**, 8561–8564.
15. Weil,D., D'Alessio,M., Raminez,F. and Eyre,D.R. (1990) Structural and functional characterization of a splicing mutation in the pro-alpha 2(I) collagen gene of an Ehlers–Danlos type VII patient. *J. Biol. Chem.*, **265**, 16007–16011.
16. Grandchamp,B., Picat,C., de Rooji,F., Beaumont,F., Wilson,P., Deybach,J.C. and Nordmann,Y. (1989) A point mutation G to A in exon 12 of the PBGD gene results in exon skipping and is responsible for acute intermittent porphyria. *Nucleic Acids Res.*, **17**, 6637–6649.
17. Carstens,R.P., Fenton,W.A. and Rosenberg,L.R. (1991) Identification of RNA splicing errors resulting in human ornithine transcarbamylase deficiency. *Am. J. Hum. Genet.* **48**, 1105–1114.
18. Marvit,J., DiLella,A.G., Brayton,K., Ledley,F.D., Robson,K.J.H. and Woo,S.L.C. (1987) GT to AT transition at a splice donor site causes skipping of the preceding exon in phenylketonuria. *Nucleic Acids Res.*, **15**, 5613–5628.
19. Hattori,M., Adachi,H., Tsujimoto,M., Arai,H. and Inoue,K. (1994) Miller–Dieker lissencephaly gene encodes a subunit of brain platelet-activating factor. *Nature*, **370**, 216–218.
20. Kornecki,E. and Ehrlich,Y.H. (1988) Neuroregulatory and neuropathological actions of the ether-phospholipid platelet-activating factor. *Science*, **240**, 1792–1794.
21. Clark,G.D., McNeil,R.S., Bix,G.J. and Swann,J.W. (1995) Platelet-Activating Factor produces neuronal growth cone collapse. *NeuroReport*, **6**, 2569–2575.
22. Fisher,E. and Scambler,P. (1994) Human haploinsufficiency, one for sorrow, two for joy. *Nature Genet.*, **7**, 5–7.
23. Kenwrick,S., Jouet,M. and Donnai,D. (1996) X Linked hydrocephalus and MASA syndrome. *J. Med. Genet.*, **33**, 59–65.
24. Brunelli,S., Faiella,A., Capra,V., Nigro,V., Simeone,A., Cama,A. and Boncinelli,E. (1996) Germline mutations in the homeobox gene *EMX2* in patients with severe schizencephaly. *Nature Genet.*, **12**, 94–96.
25. Franco,B., Guioli,S., Pragliola,A., Incerti,B., Bardoni,B., Tonlorenzi,R., Carrozzo,R., Maestrini,E., Pieretti,M., Taillon-Miller,P., Brown,C.J., Willard,H.F., Lawrence,C., Persico,M.G., Camerino,G. and Ballabio,A. (1991) A gene deleted in Kallmann's syndrome shares homology with neural cell adhesion and axonal path-finding molecules. *Nature*, **353**, 529–536.
26. Hardelin,J.-P., Levilliers,J., Blanchard,S., Carel,J.-C., Leutenegger,M., Pinard-Bertelletto,J.-P., Bouloux,P. and Petit,C. (1993) Heterogeneity in the mutations responsible for X chromosome-linked Kallmann syndrome. *Hum. Mol. Genet.*, **2**, 373–377.
27. Chomczynsky,P. and Sacchi,N. (1987) Single step method of RNA isolation by acid guanidium thiocyanate-phenol-chlorophorm extraction. *Anal. Biochem.*, **162**, 156–159.
28. Sambrook,J., Fritsch,E.F. and Maniatis,T. (1989) *Molecular Cloning: A Laboratory Manual.* 2nd ed. Cold Spring Harbor Laboratory Press, Cold Spring Harbor, NY.
29. Grace,M., Buzard,G.S. and Weintraub,B.D. (1995) Allele-Specific Associated Polymorphism analysis: novel modification of SSCP for mutation detection in heterozygous alleles using the paradigm of resistance of thyroid hormone. *Hum. Mutat.*, **6**, 232–242.